

Free-Space Optical Communication With Reconfigurable Intelligent Surfaces

Liang Yang, Wang Guo, Daniel Benevides da Costa, and Mohamed-Slim Alouini

Abstract—Despite the promising gains, free-space optical (FSO) communication is severely influenced by atmospheric turbulence and pointing error issues, which make its practical design a bit challenging. In this paper, with the aim to increase the communication coverage and improve the system performance, reconfigurable intelligent surfaces (RISs) are considered in an FSO communication setup, in which both atmospheric turbulence and pointing errors are considered. Closed-form expressions for the outage probability, average bit error rate, and channel capacity are derived assuming large number of reflecting elements at the RIS. Specifically, according to central limit theorem (CLT), while assuming multiple reflecting elements approximate expressions are proposed. It is shown that the respective accuracies increase as the number of elements at the RIS increases. Illustrative numerical examples are shown along with insightful discussions. Finally, Monte Carlo simulations are presented to verify the correctness of the analytical results.

Index Terms—Atmospheric turbulence, free-space optical communication, optical reconfigurable intelligence surface, performance analysis, pointing error.

I. INTRODUCTION

FREE-space optical (FSO) communication, usually called as outdoor optical wireless communication (OWC), has been extensively investigated in the literature along the last years due to its promising gains, such as low error rates, license free operation, and high security. In addition, FSO links can be seen as a very cost effective way to provide high bandwidth links over short distances. Potential applications to FSO communication include land and space communication, such as building-to-building, satellite-to-ground, and satellite-to-satellite communications [1]. However, FSO communications are highly affected by atmospheric attenuation and turbulence of the environment which may result in performance degradation. Moreover, pointing error is another practical issue that immensely impact the system performance of FSO links [2]. A mixed FSO-radio-frequency (RF) relaying system with energy harvesting scheme was proposed in [3].

With the commercialization of the fifth generation (5G) wireless systems, the research community has devoted the attention to the design of beyond 5G communications. Under this perspective, a new disruptive concept, called reconfigurable intelligent surface (RIS), has arisen as a promising technology to fulfill the envisaged future requirements. The RIS consists of man-made electromagnetic materials that can

intelligently control the characteristics (e.g., electromagnetic properties) of the propagation signal, such as amplitude, phase, and polarization [4-7]. Recently, the RIS has been widely studied by virtue of its advantages and harmonious integration with wireless communication systems. For instance, the RIS-assisted unmanned aerial vehicle (UAV) communication was studied in [8], the highly closed-form accurate approximations of the channel distribution of the RIS-assisted system were derived in [9], the RIS-aided system security was investigated in [10], and the RIS-assisted system coverage analysis was analyzed in [11]. In addition, similar to the deployment of the RIS in microwave band operations, the optical RIS has also attracted considerable attention since it can customize the reflecting incident beam, control the beam intensity, phase, frequency, and polarity, as well as adjust the orientation of the output beam due to user's movement [12]. In [13], a new pointing error model caused by beam jitter and intelligent channel reconfigurable node (ICRN) jitter was presented, in which a geometric and misalignment losses (GML) model was established to study the influence of size, position, and direction of the optical RIS on the FSO channel. However, they did not take the atmospheric turbulence into consideration.

In this paper, differently from previous works, we investigate the FSO communication with an optical RIS in the presence of both atmospheric turbulence and pointing errors. Closed-form expressions for the outage probability, average bit error rate (BER), and channel capacity are derived assuming large number of reflecting elements at the RIS. Specifically, due to the use of central limit theorem (CLT), while assuming multiple reflecting elements approximate expressions are proposed. It is shown that the approximations become tighter as the number of reflecting units at the RIS increases. Illustrative numerical examples are shown along with insightful discussions. Finally, Monte Carlo simulations are presented to verify the correctness of the analytical results. To the best of the authors' knowledge, such kind of system setup in conjunction to the proposed analysis have not been investigated in the literature yet.

II. SYSTEM AND CHANNEL MODELS

We assume an RIS-aided FSO communication system composed of an optical source, an optical RIS, and a destination, as shown in Fig. 1. Due to the obstruction of buildings, there is no direct link between the source and destination, with the communication being performed only through the RIS, which is placed strategically on a building to provide connectivity between source and destination. The RIS is formed by N

L. Yang and W. Guo are with the Department of College of Computer Science and Electronic Engineering, Hunan University, Changsha 410082, China, (e-mail: liangy@hnu.edu.cn, wangguo@hnu.edu.cn).

D. B. da Costa is with the Department of Computer Engineering, Federal University of Ceará, Sobral 62010-560, Brazil (email: danielbcosta@ieee.org).

M.-S. Alouini is with the CEMSE Division, King Abdullah University of Science and Technology (KAUST), Thuwal 23955-6900, Saudi Arabia (email: slim.alouini@kaust.edu.sa).

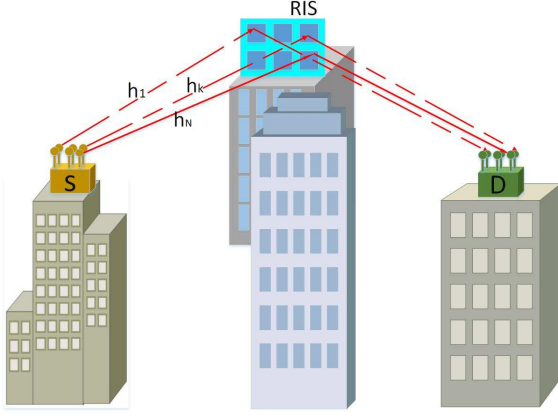


Fig. 1. Block diagram of the RIS-aided FSO communication system.

reflecting elements, while the source and destination are multi-aperture devices. The received signal at the destination is given by

$$y = \sum_{k=1}^N h_k s_k + n, \quad (1)$$

where s_k is the signal intensity with average power P_t , $h_k = h_{a_k} h_{p_k}$ is the cascaded channel from the source to the destination through the k -th reflecting element, and n is the AWGN term with zero mean and variance N_0 . Let $L_{1,k}$ and $L_{2,k}$ denote the distance between source and the RIS, and between the RIS and destination, respectively. Considering the far field case, we assume $L_{1,k} = L_1$, $L_{2,k} = L_2$ and $L_1 + L_2 = L$. Based on this assumption, all the links suffer from the independent and identically distributed (i.i.d.) fading.

A. Atmospheric Turbulence

Under atmospheric turbulence, h_{a_k} can be modeled by a Gamma-Gamma distribution which measures the moderate-to-strong atmospheric turbulence fading [14]. Thus, the probability density function (PDF) of h_{a_k} can be expressed as

$$f_{h_a}(h_{a_k}) = \frac{2(\alpha\beta)^{\frac{\alpha+\beta}{2}}}{\Gamma(\alpha)\Gamma(\beta)} h_{a_k}^{\frac{\alpha+\beta}{2}-1} K_{\alpha-\beta}(2\sqrt{\alpha\beta}h_{a_k}), \quad (2)$$

where $K_v(\cdot)$ represents the second kind of v -order modified Bessel function [15, Eq. (8.407)] and $\Gamma(\cdot)$ denotes the Gamma function [15, Eq. (8.310)]. In addition, from [14], the following parameters are determined by the atmospheric

condition: $\alpha = \left[\exp \left(\frac{0.49\sigma_R^2}{(1+0.18\kappa^2+0.56\sigma_R^{\frac{12}{5}})^{\frac{7}{6}}} - 1 \right) \right]^{-1}$

and $\beta = \left[\exp \left(\frac{0.51\sigma_R^2 \left(1 + 0.69\sigma_R^{\frac{12}{5}} \right)^{-\frac{5}{6}}}{(1+0.9\kappa^2+0.62\kappa^2\sigma_R^{\frac{12}{5}})^{\frac{7}{6}}} - 1 \right) \right]^{-1}$, where

$\sigma_R^2 = 0.5C_n^2 k_w^{\frac{7}{6}} L^{\frac{11}{6}}$ and $\kappa^2 = \frac{k_w D_a^2}{4L}$. The optical wave number can be calculated by $k_w = \frac{2\pi}{\lambda_w}$, the wavelength is expressed by λ_w , the diameter of the receiver aperture is denoted by $D_a = 2a$, and C_n^2 means the index of the refractive parameter.

B. Pointing Error

Pointing error is affected by the beam jitter and ICRN jitter [12], where the beam jitter means that the beam vibrates due to the jitter at the transmitter and ICRN jitter refers to the normal vector deflection of reflection surface caused by the jitter of the ICRN surface. For a single intelligent optical channel, the pointing error model has been described in [Figs. 2 and 3, 12], where the superimposed pointing error angle θ'_k is the angle between the ICRN reflection point and the actual incident point at the receiver, and it can be modeled by a Rayleigh distribution. In addition, θ'_k can be computed by $\theta'_k = \sqrt{\theta'_{x_k}{}^2 + \theta'_{y_k}{}^2}$ [12], where $\theta'_{x_k} \approx \left(1 + \frac{L_1}{L_2}\right) \theta_{x_k} + 2\beta_{x_k}$ and $\theta'_{y_k} \approx \left(1 + \frac{L_1}{L_2}\right) \theta_{y_k} + 2\beta_{y_k}$, with $\{\theta_{x_k}, \theta_{y_k}\} \sim \mathcal{N}(0, \sigma_\theta^2)$ and $\{\beta_{x_k}, \beta_{y_k}\} \sim \mathcal{N}(0, \sigma_\beta^2)$, where $\sim \mathcal{N}(\mu, \sigma^2)$ indicates a Normal distribution with mean μ and variance σ^2 . The PDF of θ'_k can be written as

$$f_{\theta'_k}(\theta'_k) = \frac{\theta'_k}{\left(1 + \frac{L_1}{L_2}\right) \sigma_\theta^2 + 4\sigma_\beta^2} e^{-\frac{\theta'^2_k}{2\left(1 + \frac{L_1}{L_2}\right) \sigma_\theta^2 + 8\sigma_\beta^2}}. \quad (3)$$

From [12], the distance r_k from the center of the receiver to the receiving spot can be expressed as $r_k = \tan\theta'_k L_2 \approx \theta'_k L_2$. Therefore, the channel fading caused by pointing error can be approximated by $h_{p_k} \approx A_0 \exp\left(-\frac{2r_k^2}{\omega_{zeq}^2}\right)$, where $A_0 = \text{erf}^2(\nu)$, $\omega_{zeq}^2 = \omega_z^2 \frac{\sqrt{\pi} \text{erf}(\nu)}{2\nu e^{-\nu^2}}$, $\text{erf}(\cdot)$ denotes the error function [15, Eq. (8.25)], $\nu = \sqrt{\frac{\pi}{2}} \frac{a}{\omega_z}$ represents the ratio of aperture radius to beam width, ω_z denotes the beam width and can be computed as $\omega_z = \phi L$, and ϕ stands for the divergence angle of the beam. Thus, the PDF of h_{p_k} can be expressed as

$$f_{h_{p_k}}(h_{p_k}) = \frac{c}{A_0} \left(\frac{h_{p_k}}{A_0} \right)^{c-1}, \quad 0 < h_{p_k} < A_0, \quad (4)$$

where

$$c = \frac{\omega_{zeq}^2}{4\sigma_\theta^2 L^2 + 16\sigma_\beta^2 L_2^2}. \quad (5)$$

C. Statistical Distribution

As mentioned in [12], it is assumed that the transmitter transmits signals to N RISs, and each RIS directly reflects the signals to the receiver. All beams are centered on the receiver, and the receiver receives all the energy of the beam. Thus, the instantaneous SNR can be formulated as

$$\gamma = \sum_{k=1}^N \gamma_k = \bar{\gamma} \sum_{k=1}^N h_k^2 = \bar{\gamma} Z, \quad (6)$$

where γ_k means the instantaneous SNR of the k -th channel and $\bar{\gamma} = \frac{P_t}{N_0}$ denotes the average SNR..

From [14], the PDF of $B = h_k^2$ can be obtained as

$$f_B(x) = \frac{\alpha\beta c}{2\sqrt{x}\Gamma(\alpha)\Gamma(\beta)A_0} \times G_{1,3}^{3,0} \left[\frac{\alpha\beta\sqrt{x}}{A_0} \middle| c-1, \alpha-1, \beta-1 \right], \quad (7)$$

where $G_{\cdot,\cdot}(\cdot)$ denotes the Meijer's G-function [16, Eq. (07.34.02.0001.01)]. Thus, the mean and variance of B can be expressed as

$$m_1 = E[B] = \frac{cA_0^2 \Gamma(c+2) \Gamma(\alpha+2) \Gamma(\beta+2)}{\alpha^2 \beta^2 \Gamma(\alpha) \Gamma(\beta) \Gamma(c+3)}, \quad (8)$$

$$\delta_1^2 = \text{VAR}[B] = \frac{cA_0^4 \Gamma(c+4) \Gamma(\alpha+4) \Gamma(\beta+4)}{\alpha^4 \beta^4 \Gamma(\alpha) \Gamma(\beta) \Gamma(c+5)} - m_1^2. \quad (9)$$

From (7), the PDF of γ_k can be written as

$$f_{\gamma_k}(\gamma) = \frac{\alpha\beta c}{2\sqrt{\gamma}\sqrt{\gamma}\Gamma(\alpha)\Gamma(\beta)A_0} \times G_{1,3}^{3,0} \left[\frac{\alpha\beta}{A_0} \sqrt{\frac{\gamma}{\gamma}} \middle| \begin{matrix} c \\ c-1, \alpha-1, \beta-1 \end{matrix} \right]. \quad (10)$$

Using (10) to evaluate the system performance is very difficult. On the basis of the CLT [17] and assuming large N , Z can be well-approximated by a Gaussian random variable with mean value equals to $m = m_1 \times N$ and variance given by $\delta^2 = \delta_1^2 \times N$. Thus, the PDF of γ can be written as

$$f_{\gamma}(x) \approx \frac{1}{\sqrt{2\pi\delta^2\gamma}} e^{-\frac{(x-\gamma m)^2}{2\gamma^2\delta^2}}. \quad (11)$$

Relying on [15, Eq. (3.322.2)] and performing the appropriate substitutions, the moment generating function (MGF), which is defined by $M_{\gamma}(s) = E[e^{-s\gamma}]$, with $E[\cdot]$ denoting expectation, can be derived as

$$M_{\gamma}(s) \approx \frac{1}{2} e^{\frac{\gamma^2 \delta^2 s}{2} - \frac{m^3}{2\delta^2} - \frac{\gamma m}{2}} \left[1 - \Phi \left(\frac{s\gamma\delta}{\sqrt{2}} - \frac{m}{2\delta} \right) \right], \quad (12)$$

where $\Phi(\cdot) = \text{erf}(\cdot)$.

In addition, from (11) and [15, Eq. (3.462.1)], the generalized moments of γ , which is given by $E[\gamma^n] = \int_0^\infty \gamma^n f_{\gamma}(\gamma) d\gamma$, can be derived as

$$E[\gamma^n] \approx \frac{\gamma^n \delta^n}{\sqrt{2\pi}} e^{\frac{-m^2}{4\delta^2}} \Gamma(n+1) D_{-n-1} \left(-\frac{m}{\delta} \right), \quad (13)$$

where $D_v(\cdot)$ is the parabolic cylinder functions.

Finally, from (13), the n -order amount of fading (AF), which is defined as $AF_{\gamma}^{(n)} = \frac{E[\gamma^n]}{E[\gamma]^n} - 1$ and arises as an important index to measure the system performance, can be obtained as

$$AF_{\gamma}^{(n)} \approx \frac{\delta^n}{\sqrt{2\pi} m^n} \Gamma(n+1) e^{-\frac{m^2}{4\delta^2}} D_{-n-1} \left(-\frac{m}{\delta} \right) - 1. \quad (14)$$

III. PERFORMANCE ANALYSIS

In this section, the outage probability, BER, and channel capacity are derived as important indexes to measure the system performance.

A. Outage Probability

Outage probability can be defined as the probability that the instantaneous SNR falls below a given threshold γ_{th} , being mathematically formulated as

$$P_{out} = \Pr(\gamma \leq \gamma_{th}) = \int_0^{\gamma_{th}} f_{\gamma}(\gamma) d\gamma. \quad (15)$$

From [15, Eqs. (2.322.1) and (2.322.2)], one can get the outage probability by integrating (15) as

$$P_{out} \approx \frac{1}{2} \left[\Phi \left(\frac{\gamma_{th} - m\bar{\gamma}}{\sqrt{2}\bar{\gamma}\delta} \right) - \Phi \left(-\frac{m}{\sqrt{2}\delta} \right) \right]. \quad (16)$$

In order to get further insights to the outage performance, asymptotic outage analysis is now carried. By setting $\bar{\gamma} \rightarrow \infty$, (10) can be written as [16, Eq.(07.34.06.0006.01)]

$$f_{\gamma_k}(\gamma) \rightarrow \sum_{i=1}^3 \frac{\prod_{j=1, j \neq i}^3 \Gamma(b_j - b_i)}{\Gamma(c - b_i)} \left(\frac{\alpha\beta}{A_0} \sqrt{\frac{\gamma}{\bar{\gamma}}} \right)^{b_i}, \quad (17)$$

where $b_i = (c-1, \alpha-1, \beta-1)$.

Similar [3], $f_{\gamma}(\gamma)$ is determined by the minimum value of $\varrho = \min(b_i)$. Then, similar to (12), we can obtain the MGF of γ_k

$$M_{\gamma_k}(s) \rightarrow \frac{\epsilon c \alpha^{1+\varrho} \beta^{1+\varrho} \Gamma\left(\frac{1+\varrho}{2}\right)}{2\Gamma(\alpha)\Gamma(\beta)A_0^{1+\varrho}(\bar{\gamma}s)^{\frac{1+\varrho}{2}}}, \quad (18)$$

where ϵ is the coefficient of the $\left(\frac{\alpha\beta}{A_0} \sqrt{\frac{\gamma}{\bar{\gamma}}}\right)^{\varrho}$. According to the relationship of $M_{\gamma}(s) = (M_{\gamma_k}(s))^N$ [12, Eq.(33)], $f_{\gamma}(\gamma) = \int_0^\infty e^{s\gamma} M_{\gamma}(s) ds$ and (15), the outage probability can be asymptotically written as

$$P_{out} \rightarrow \left(\frac{\epsilon c \alpha^{1+\varrho} \beta^{1+\varrho} \Gamma\left(\frac{1+\varrho}{2}\right)}{2\Gamma(\alpha)\Gamma(\beta)A_0^{1+\varrho}\bar{\gamma}^{\frac{1+\varrho}{2}}} \right)^N \times \frac{\gamma_{th}^{\frac{(1+\varrho)N}{2}}}{\Gamma\left(\frac{(1+\varrho)N}{2}\right) \frac{(1+\varrho)N}{2}}, \quad (19)$$

which indicates that the diversity order equals to $\frac{(1+\varrho)N}{2}$. Therefore, increasing N can improve the system performance.

B. Average BER

For most binary correlated modulation schemes, the average BER can be calculated by the following expression [17]

$$Pe = \int_0^\infty Q\left(\sqrt{2\psi\gamma}\right) f_{\gamma}(\gamma) d\gamma, \quad (20)$$

where $Q(\cdot)$ denotes the Q-function [15, Eq. (6.287.3)], and ψ represents a coefficient applied to different modulation methods. For example, $\psi = 1$ for binary phase shift keying (BPSK), $\psi = 0.5$ for coherent detection of binary frequency keying (BFSK), and $\psi = 0.75$ for coherent detection of minimum shift keying [18].

From [19, Eq.(14)] and [15, Eq.(6.287)], the Q-function can be approximately expressed as $Q(x) = \frac{1}{2} \text{erfc}\left(\frac{x}{\sqrt{2}}\right) \simeq \frac{1}{12} e^{-\frac{x^2}{2}} + \frac{1}{4} e^{-\frac{2x^2}{3}}$. Considering the BPSK modulation scheme and making use of [15, Eqs. (2.322.1) and (2.322.2)], we obtain

$$Pe \approx \frac{1}{12} \frac{\sqrt{\pi\rho} e^{-\frac{m^2}{2\delta^2}}}{\sqrt{2\pi\delta^2\bar{\gamma}}} e^{\rho\epsilon^2} (1 - \Phi(\epsilon\sqrt{\rho})) + \frac{1}{4} \frac{\sqrt{\pi\rho} e^{-\frac{m^2}{2\delta^2}}}{\sqrt{2\pi\delta^2\bar{\gamma}}} e^{\rho\iota^2} (1 - \Phi(\iota\sqrt{\rho})), \quad (21)$$

where $\epsilon = 1 - \frac{m}{\bar{\gamma}\delta^2}$, $\iota = \frac{4}{3} - \frac{m}{\bar{\gamma}\delta^2}$, $\rho = \frac{\bar{\gamma}^2\delta^2}{2}$.

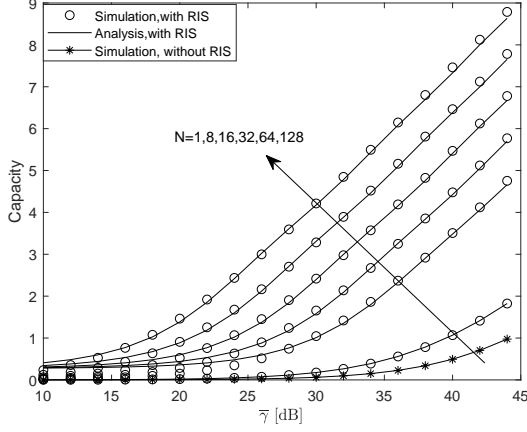


Fig. 2. Channel capacity of the RIS-aided FSO system for different values of N .

C. Channel Capacity

For the channel capacity, it can be calculated as [20]

$$C = \int_0^\infty \log_2(1+x) f_\gamma(x) dx. \quad (22)$$

From [21], it is shown that $\log_2(1+x)$ can be well-approximated by $\log_2(1+x) \approx \sum_{i=1}^4 \eta_i e^{-\zeta_i x}$, where $\eta = [9.331, -2.635, -4.032, -2.388]$ and $\zeta = [0.000, 0.037, 0.004, 0.274]$. Then, the channel capacity can be derived as

$$C \approx \frac{1}{2} e^{-\frac{m^2}{2\delta^2}} \sum_{i=1}^4 \eta_i e^{\frac{\gamma^2 \delta^2}{2} (\zeta_i - \frac{m}{\gamma \delta^2})^2} \times \left[1 - \Phi \left(\frac{\zeta_i \bar{\gamma} \delta}{\sqrt{2}} - \frac{m}{\sqrt{2} \delta} \right) \right]. \quad (23)$$

IV. NUMERICAL RESULTS AND DISCUSSIONS

In this section, representative numerical results are provided to illustrate the performance of the RIS-aided FSO communication system. The impact of the key system parameters on the system performance is investigated. Monte Carlo simulations are also presented to corroborate the proposed analysis and derived expressions. Unless otherwise stated, we have considered in the plots the following parameters: $\sigma_\theta = 1$ mrad, $\sigma_\beta = 0.5$ mrad, $w_z = 120$ cm, $a = 10$ cm, $\alpha = 15$, $\beta = 10$, $L_1 = L_2 = 150$ m [12]. In addition, when a single path (direct link, without RIS) is considered, we set the path distance as $L = 100$ m and the standard deviation of pointing error angle as $\sigma_\theta = 1$ mrad.

In Fig. 2, the channel capacity versus $\bar{\gamma}$ is plotted for different values of N . Note that although the path distance when $N = 1$ is 300 m, its capacity performance slightly improves under high SNR regime when compared with the direct link assuming 100 m as path distance. Observe also that the capacity performance significantly improves as N increases.

Fig. 3 plot the outage probability, versus $\bar{\gamma}$ for different values of ω_z and a . We set $N = 128$ and the other parameters are consistent with those of Fig. 2. Similar conclusions to

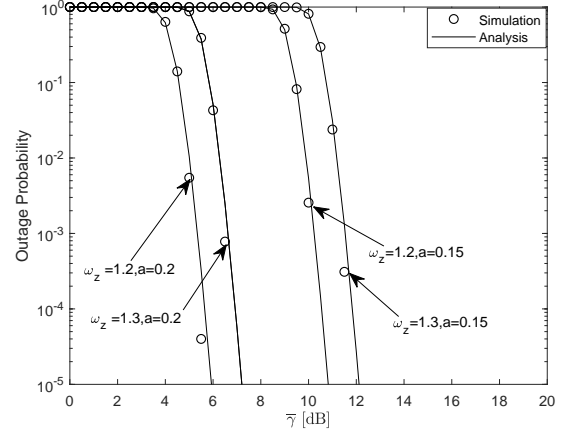


Fig. 3. Outage probability of the RIS-aided FSO systems for different values of ω_z and a .

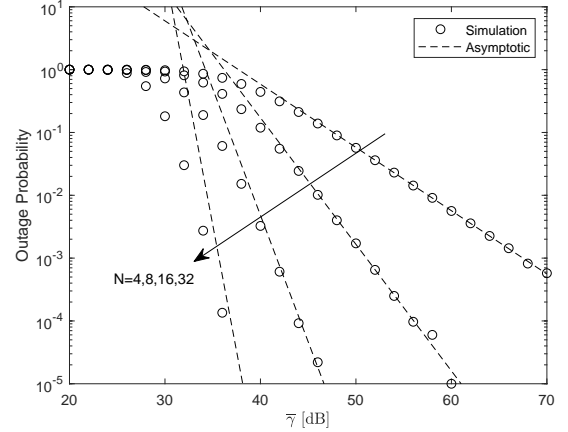


Fig. 4. Outage probability of the RIS-aided FSO system for different values of N ($\alpha = 6.5$, $\beta = 6.0$, $\sigma_\theta = 20$ mrad, $\sigma_\beta = 20$ mrad, and $c = 0.5$).

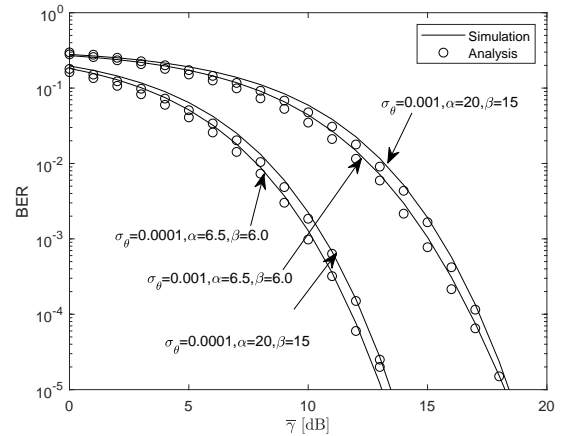


Fig. 5. BER of the RIS-aided FSO system for different values of α , β , and σ_θ .

those ones attained in Fig. 2 are attained. In addition, it can be observed that the outage performance can be improved by decreasing the value of $\frac{w_s}{a}$. Fig. 4 plots the asymptotic outage curves, which shows that the diversity order increases with N , corroborating our analysis.

Finally, the effect of different system parameters (e.g., α , β , and σ_θ) on the BER performance is studied in Fig. 5. We set $L_1 = 350$ m, $L_2 = 250$ m, $N = 128$, $a = 20$ cm. It can be clearly seen that the BER probability under strong turbulence is better than that of under moderate turbulence. In addition, with the change of atmospheric turbulence, the BER performance is slightly affected. One can also see that σ_θ has a great impact in the performance, i.e., when the value of σ_θ increases, the BER becomes worse.

V. CONCLUSION

In this paper, a FSO system aided by RISs was investigated. Closed-form expressions for the outage probability, average BER, and channel capacity were derived. It was shown that the deployment of RISs can significantly improve the performance of FSO communication systems. In addition, our results reveal that pointing error has a great impact on the system performance when compared with the atmospheric turbulence.

REFERENCES

- [1] H. Kaushal and G. Kaddoum, "Optical communication in space: challenges and mitigation techniques," *IEEE Commun. Surveys Tuts.*, vol. 19, no. 1, pp. 57-96, Firstquarter 2017.
- [2] M. A. Khalighi and M. Uysal, "Survey on free space optical communication: a communication theory perspective," *IEEE Commun. Surveys Tuts.*, vol. 16, no. 4, pp. 2231-2258, Fourthquarter 2014.
- [3] J. Chen et al., "A novel energy harvesting scheme for mixed FSO-RF relaying systems," *IEEE Trans. Veh. Technol.*, vol. 68, no. 8, pp. 8259-8263, Aug. 2019.
- [4] M. Di Renzo et al., "Smart radio environments empowered by reconfigurable intelligent surfaces: how it works, state of research, and road ahead," *IEEE J. Sel. Areas Commun.*, DOI: 10.1109/JSAC.2020.3007211.
- [5] E. Basar, M. Di Renzo, J. De Rosny, M. Debbah, M. Alouini, and R. Zhang, "Wireless communications through reconfigurable intelligent surfaces," *IEEE Access*, vol. 7, pp. 116753-116773, 2019.
- [6] W. Tang, M. Chen, X. Chen, J. Dai, Y. Han, M. Renzo, Y. Zeng, S. Jin, Q. Cheng, T. Cui, "Wireless communications with reconfigurable intelligent surface: path loss modeling and experimental measurement," [Online]. Available: <https://arxiv.org/abs/1911.05326>.
- [7] Y. Yuan, Y. Zhao, B. Zong, et al. "Potential key technologies for 6G mobile communications," *Sci. China Inf. Sci.*, 63, 183301 (2020).
- [8] L. Yang, F. Meng, J. Zhang, M. O. Hasna, and M. Di Renzo, "On the performance of RIS-assisted dual-hop UAV communication systems," *IEEE Trans. Veh. Technol.*, DOI: 10.1109/TVT.2020.3004598.
- [9] L. Yang, F. Meng, Q. Wu, D. B. da Costa, and M. Alouini, "Accurate closed-form approximations to channel distributions of RIS-aided wireless systems," *IEEE Wireless Commun. Lett.*, DOI: 10.1109/LWC.2020.3010512.
- [10] L. Yang, J. Yang, W. Xie, M. O. Hasna, T. Tsiftsis, and M. Di Renzo, "Secrecy performance analysis of RIS-aided wireless communication systems," *IEEE Trans. Veh. Technol.*, DOI: 10.1109/TVT.2020.3007521.
- [11] L. Yang, Y. Yang, M. O. Hasna, and M. Alouini, "Coverage, probability of SNR gain, and DOR analysis of RIS-aided communication systems," *IEEE Wireless Commun. Lett.*, vol. 9, no. 8, pp. 1268-1272, Aug. 2020.
- [12] H. Wang, Z. Zhang, B. Zhu, J. Dang, L. Wu, L. Wang, K. Zhang, Y. Zhang, "Performance of wireless optical communication with reconfigurable intelligent surfaces and random obstacles," [Online]. Available: <https://arxiv.org/abs/2001.05715>.
- [13] M. Najafi, B. Schmauss, R. Schobe, "Intelligent reconfigurable reflecting surfaces for free space optical communication," [Online]. Available: <https://arxiv.org/abs/2005.04499>.
- [14] W. Gappmair, "Further results on the capacity of free-space optical channels in turbulent atmosphere," *IET Commun.*, vol. 5, no. 9, pp. 1262-1267, Jun. 2011.
- [15] I. S. Gradshteyn and I. M. Ryzhik, *Table of integrals, series and products*, 7th ed. San Diego, CA, USA: Academic, 2007.
- [16] Wolfram, The Wolfram functions site, Available: <http://functions.wolfram.com>.
- [17] J. G. Proakis, *Digital Communications*, 5th ed. New York: McGrawHill, 2008.
- [18] A. M. Magableh and M. M. Matalgah, "Moment generating function of the generalized α - μ distribution with applications," *IEEE Commun. Lett.*, vol. 13, no. 6, pp. 411-413, Jun. 2009.
- [19] M. Chiani, D. Dardari, and M. K. Simon, "New exponential bounds and approximations for the computation of error probability in fading channels," *IEEE Trans. Wireless Commun.*, vol. 2, no. 4, pp. 840-845, Jul. 2003.
- [20] A. J. Goldsmith and P. P. Varaiya, "Capacity of fading channels with channel side information," *IEEE Trans. Inf. Theory*, vol. 43, no. 6, pp. 1986-1992, Nov. 1997.
- [21] E. Salahat and A. Hakam, "Novel unified expressions for error rates and ergodic channel capacity analysis over generalized fading subject to AWGGN," *2014 IEEE GCC*, Austin, TX, 2014, pp. 3976-3982.